

Improvement the DTC System for Electric Vehicles Induction Motors

Ali Arif¹, Achour Betka², Abderezak Guettaf³

Abstract: A three-phase squirrel-cage induction motor is used as a propulsion system of an electric vehicle (EV). Two different control methods have been designed. The first is based on the conventional DTC Scheme adapted for three-level inverter. The second is based on the application of fuzzy logic controller to the DTC scheme. The motor is controlled at different operating conditions using a FLC based DTC technique. In the simulation the novel proposed technique reduces the torque and current ripples. The EV dynamics are taken into account.

Keywords: Electric vehicle, Induction motor, FLC based DTC scheme.

1 Introduction

Many control techniques have been applied on induction motors [1, 2]. Among these techniques, DTC appears to be very convenient for EV applications [3]. This control strategy was introduced by Takahaschi [4]. Most of the literature is focused on the application of DTC with two-level inverters. But DTC with multilevel inverters is still a matter of research [5-9]. The present work is based on the study of the application of DTC to the three-level NPC inverter, and the advantages that can be obtained. When using a three-level inverter the selection of the output voltage vector becomes more complex due to the higher number of available inverter states. Two different control methods have been designed. The first is based on the conventional DTC scheme adapted for three-level inverter. The second is based on fuzzy logic controller introduced to replace the conventional table used in DTC for the inverter state selection. The required measurements for this control technique are only the voltage and the current measurements. Flux, torque, and speed are estimated. The input of the motor controller is the reference speed, which is directly applied by the pedal of the vehicle.

In this paper a detailed dynamic model of an EV is introduced and associated with the proposed FLC based DTC induction motor drive strategy.

¹Electrical engineering Department, University of Biskra, BP: 156, Algeria; E-mail: aelectrot@yahoo.fr

²Electrical engineering Department, University of Biskra, BP: 156, Algeria; E-mail: a_Betka@hotmail.com

³Electrical engineering Department, University of Biskra, BP: 156, Algeria; E-mail: a_Guettaf@yahoo.fr

The objective is to test the performance of the proposed control strategy on the whole vehicle and not on the sole induction motor.

2 Vehicle Dynamics Analysis

2.1 Dynamics analysis

Based on principles of vehicle dynamics and aerodynamics [10-12], the road load F_w can be described with accuracy via (1). It consists of rolling resistance, f_r , aerodynamic drag, f_{ad} and climbing resistance, f_{rs} :

$$F_w = f_r + f_{ad} + f_{rs} . \quad (1)$$

The rolling resistance (f_r) is caused by the tire deformation on the road:

$$f_r = f m g , \quad (2)$$

where f is the tire rolling resistance coefficient. It increases with vehicle velocity, and also during vehicle turning manoeuvres.

Aerodynamic drag (f_{ad}) is the viscous resistance of air acting upon the vehicle, given as:

$$f_{ad} = 0,5\xi C_w A(v + v_0)^2 . \quad (3)$$

It increases with square of the vehicle speed v , and depends on the front area A .

The climbing resistance (f_{rs}) with positive operational (sign) and the down grade force (f_{rs}) with negative operational (sign) is given by

$$f_{rs} = m g \sin \alpha , \quad (4)$$

where m is the total mass of the vehicle, g is the gravitational acceleration constant and α is the grade angle. The forces acting on the vehicle are shown in Fig. 1.

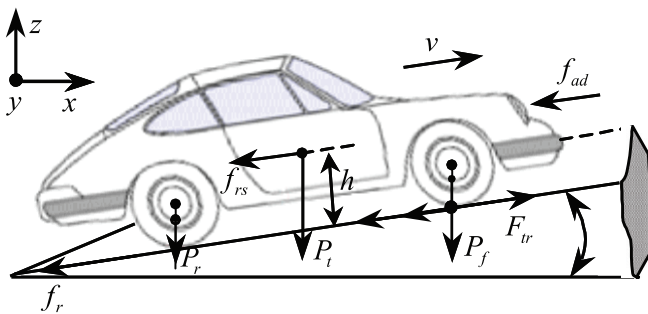


Fig. 1 – Forces acting on vehicle.

The motive force, F_{tr} , available from the propulsion system is partially consumed in overcoming the road load, F_w . The net force ($F_{tr} - F_w$) accelerates the vehicle (or decelerates when F_w exceeds F_{tr}). The torque of the motor together with the electric vehicle load can be written as:

$$T_{em} = J \frac{d\omega}{dt} + B\omega + T_{ev}, \quad (5)$$

where ω is the angular velocity of the rotor in rad/s, J is the moment of inertia of the system, and B is the viscous coefficient of the motor. T_{em} describes the electromagnetic motor torque and T_{ev} is the electric vehicle torque which can be obtained from the tractive force F_{tr} and wheel radius r_{wh} of the vehicle as:

$$T_{ev} = F_{tr} r_{wh}. \quad (6)$$

2.2 Induction motor model

The unsaturated induction motor model in the stator-fixed d-q reference frame can be expressed as:

$$\begin{aligned} V_s &= R_s I_s + \frac{d}{dt} \Phi_s, \\ V_r &= R_r I_r + \frac{d}{dt} \Phi_r - j\omega_r \Phi_r, \\ \Phi_s &= L_s I_s + L_m I_r, \\ \Phi_r &= L_r I_r + L_m I_s. \end{aligned} \quad (7)$$

The induction motor stator flux can be estimated as follows:

$$\left\{ \begin{aligned} \Phi_{ds} &= \int (V_{ds} - R_s I_{ds}) dt, \\ \Phi_{qs} &= \int (V_{qs} - R_s I_{qs}) dt, \\ |\Phi_s| &= \sqrt{\Phi_{ds}^2 + \Phi_{qs}^2}, \\ \theta_s &= \arctg \frac{\Phi_{qs}}{\Phi_{ds}}. \end{aligned} \right. \quad (8)$$

Equation (8) performs a good estimation of ϕ_s at high speed. The motor electromagnetic torque is given as:

$$T_{em} = \frac{3}{2} \frac{P}{2} (\varphi_{ds} I_{qs} - \varphi_{qs} I_{ds}). \quad (9)$$

Equation (9) is used to estimate T_{em} during the simulation process.

2.3 NPC three-level inverter topology

Different circuit topologies have been implemented in multilevel inverter [6, 13]. One of the most used of these topologies is the neutral Point Clamped (NPC) topology. (Fig. 2) presents the schematic diagram of a three- level NPC inverter.

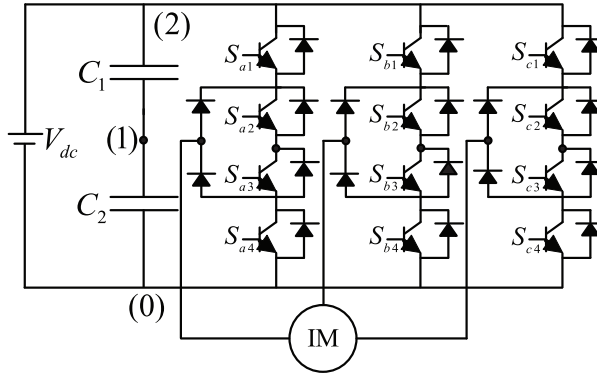


Fig. 2 – Three-level NPC inverter.

The representation of the space voltage vectors of the three-level inverter for all switching states is depicted in Fig. 3. We divide them into four groups [14]: Small voltages vectors: $v_{13}, v_{14}, v_{15}, v_{16}, v_{17}, v_{18}$; Medium voltages vectors: $v_2, v_4, v_6, v_8, v_{10}, v_{12}$; Large voltages vectors: $v_1, v_3, v_5, v_7, v_9, v_{11}$ and zero voltages vectors: v_0 .

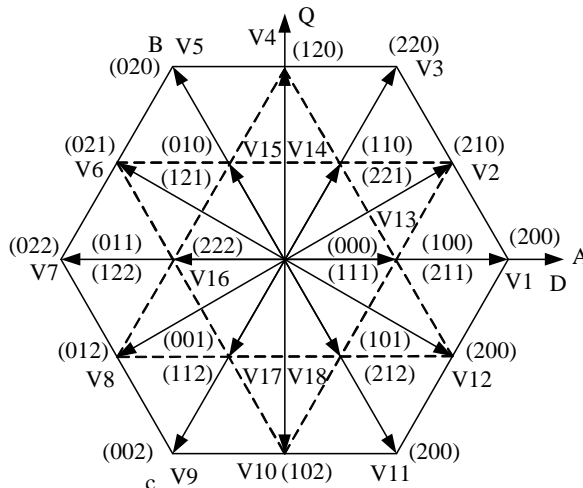


Fig. 3 – Space voltage vectors of three-level inverter.

The zero voltage vector (ZVV) has three switching state, the small voltage vector (SVV) has two and both the medium voltage vector (MVV) and the large voltage vector (LVV) have only one.

3 Proposed Approach

The control command for the system is speed (by means of the pedal). The flux reference can be calculated based on the speed. The reference torque can be calculated using the difference between reference speed and rated speed (using a PI controller). Two hysteresis controllers (Fig. 4) are used to control torque and flux. Flux and torque errors are calculated as follows:

$$\begin{aligned} E_{\Phi} &= \Phi_s^* - \Phi_s, \\ E_t &= T_e^* - T_e, \end{aligned} \quad (10)$$

where Φ_s^* and T_e^* are the reference flux and torque, respectively.

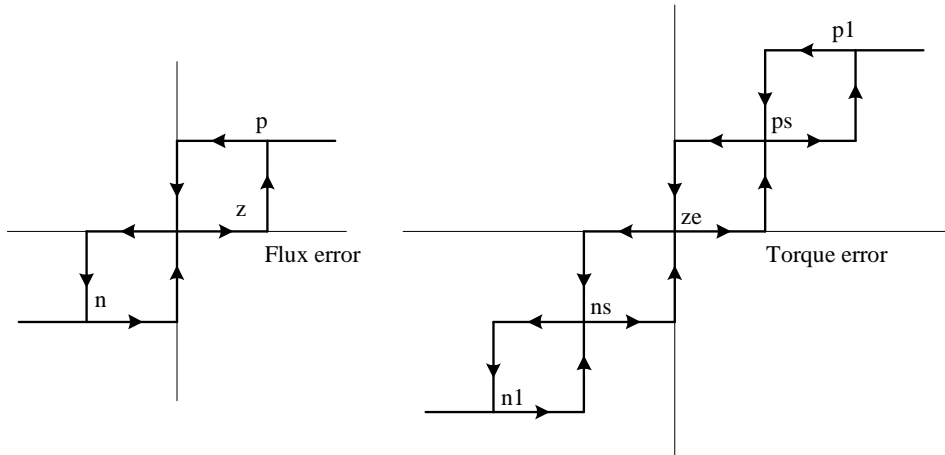


Fig. 4 – Hysteresis blocks of DTC with a three-level NPC inverter
 (n: flux decrease; z: flux equal; p: flux increase; n₁: torque high decrease;
 n_s: torque decrease; z_e: torque equal; p_s: torque increase; p₁: torque high increase).

To perform the conventional DTC control applied to a three-level, the stator flux position has been divided into 12 sectors of 30° degrees. The **Table 1** for the inverter state selection has been devised to achieve an accurate control of both torque and stator flux and reduce the torque ripple inherent in the DTC method. The numbers in the table for the output voltage vector or inverter state are written according to Fig. 3. The conventional DTC for three-level inverter using the hysteresis based voltage switching method has relative merits of simple structure and easy implementation. If the dynamic of an electric vehicle

is introduced and associated with the proposed control, DTC advantages are not sufficient. Therefore, the application of a fuzzy logic controller to the direct torque controls [15-17] so as to minimize the torque ripple and to maximize the drive efficiency. The major problem with switching table based DTC drive is high torque and current ripples. To increase traditional DTC of induction motor control precision and decrease large torque ripple, a fuzzy DTC control system is proposed. Fig. 5 shows the control scheme with the fuzzy logic controller which modifies the DTC by incorporating fuzzy logic into it.

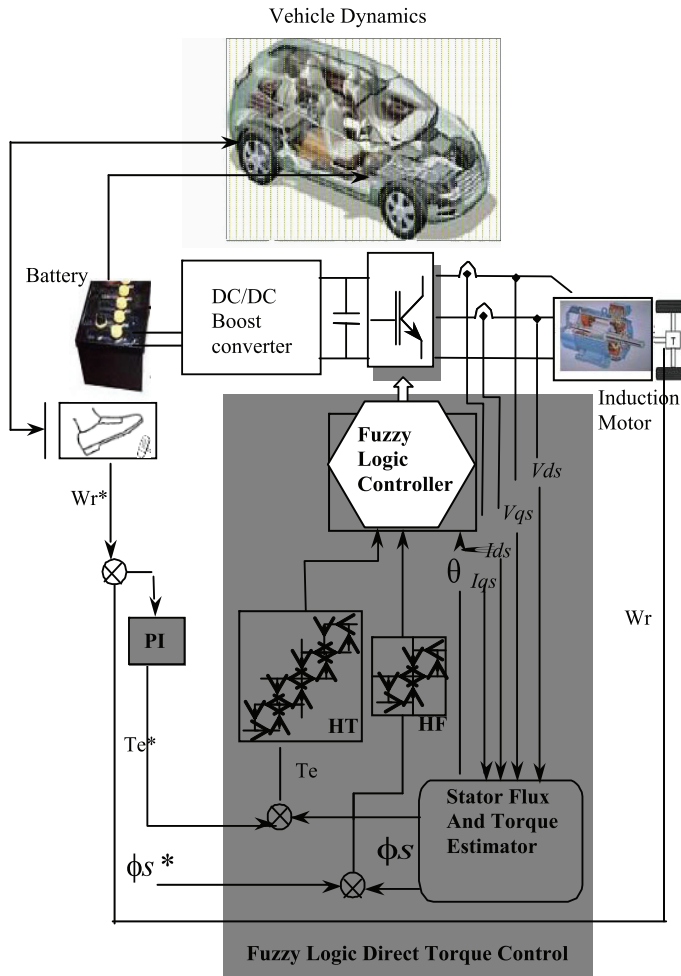


Fig. 5 – The control scheme with the fuzzy logic Controller.

The fuzzy controller is designed to have three fuzzy state variables and one control variable. Each variable is divided into fuzzy segments. The number of fuzzy segments in each variable is chosen to have maximum control with minimum number of rules. The first variable is E_ϕ (stator flux error). The linguistic terms used for the stator flux error are: E_{ϕ_n} (negative error), E_{ϕ_z} (zero error), and E_{ϕ_p} (positive error). The membership function for the stator flux error is shown in Fig. 6a which uses a triangular distribution. The second fuzzy state variable is E_t (torque error). The linguistic terms used for the torque error are: $E_{t_{nl}}$ (negative large error), $E_{t_{nz}}$ (negative small error), E_{t_z} (zero error), $E_{t_{ps}}$ (positive small error) and $E_{t_{pl}}$ (positive large error). The membership function for the torque error is given in Fig. 6b. The third fuzzy state variable is the stator flux position θ . In order to achieve a more accurate selection of the inverter state, the stator flux position has been divided into 12 sectors. The universe of discourse of this variable has been divided into twelve fuzzy sets (θ_1 to θ_{12}), the membership distribution is shown in Fig. 6c.

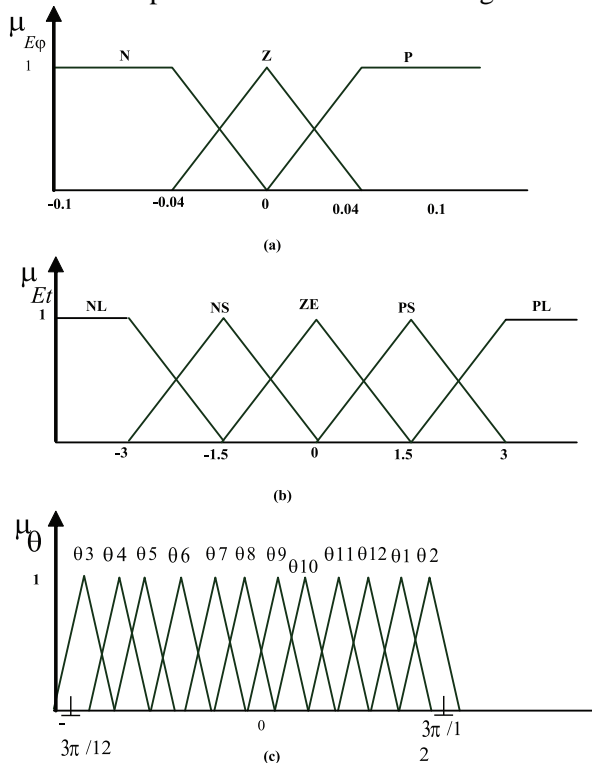


Fig. 6 – Membership functions for the inputs (a): Stator flux error; (b): Torque error; (c): Stator flux position.

The control variable is the inverter state n . In a three-level inverter, 27 switching states are possible. The definition of membership distribution is not necessary for the output variable. The control rule, can be described using the state variables E_ϕ , E_t , θ and the control variables n . The i^{th} rule R_i can be written as:

$$R_i : \text{if } E_\phi \text{ is } A_i, E_t \text{ is } B_i, \theta \text{ is } C_i, \text{ then } n \text{ is } N_i,$$

where A_i , B_i , C_i , and N_i represent the fuzzy segments.

The total number of rules is 180 as shown in **Table 1**.

Table 1
Vector selection table.

θ_1				θ_2				θ_3				θ_4			
E_t E_ϕ	P	Z	N												
PL	V0	V0	V0												
PS	V15	V14	V14	PS	V16	V15	V15	PS	V16	V15	V15	PS	V17	V16	V16
ZE	V15	V14	V14	ZE	V16	V15	V15	ZE	V16	V15	V15	ZE	V17	V16	V16
NS	V5	V4	V3	NS	V6	V5	V5	NS	V7	V6	V5	NS	V8	V7	V7
NL	V5	V4	V3	NL	V6	V5	V5	NL	V7	V6	V5	NL	V8	V7	V7
θ_5				θ_6				θ_7				θ_8			
E_t E_ϕ	P	Z	N												
PL	V0	V0	V0												
PS	V17	V16	V16	PS	V18	V17	V17	PS	V18	V17	V17	PS	V13	V18	V18
ZE	V17	V16	V16	ZE	V18	V17	V17	ZE	V18	V17	V17	ZE	V13	V18	V18
NS	V9	V8	V7	NS	V10	V9	V9	NS	V11	V10	V9	NS	V12	V11	V11
NL	V9	V8	V7	NL	V10	V9	V9	NL	V11	V10	V9	NL	V12	V11	V11
θ_9				θ_{10}				θ_{11}				θ_{12}			
E_t E_ϕ	P	Z	N												
PL	V0	V0	V0												
PS	V13	V18	V18	PS	V14	V13	V13	PS	V14	V13	V13	PS	V15	V14	V14
ZE	V13	V18	V18	ZE	V14	V13	V13	ZE	V14	V13	V13	ZE	V15	V14	V14
NS	V1	V12	V11	NS	V2	V1	V1	NS	V3	V2	V1	NS	V4	V3	V3
NL	V1	V12	V11	NL	V2	V1	V1	NL	V3	V2	V1	NL	V4	V3	V3

Each cell shows the best switching state for the given angle. The interface method used is basic and simple and is developed from the minimum operation rule as a fuzzy implementation function. The membership functions of A , B , C and N are given by μA , μB , μC , and μN respectively. The firing strength of i^{th} rule α_i can be expressed as:

$$\alpha_i = \min(\mu A_i(E_\phi), \mu B_i(E_t), \mu C_i(\theta)). \quad (11)$$

By fuzzy reasoning using Mamdani's minimum operation rule as a fuzzy implication function, the i^{th} rule leads to the control decision

$$\mu_{N_i}(n) = \min(\alpha_i, \mu_{N_i}(n)). \quad (12)$$

Thus the membership function μ_N of the output n is point wise given by:

$$\mu_N(n) = \max_{i=1}^{180}(\mu'_{N_i}(n)). \quad (13)$$

Since the output is crisp, the maximum criterion method is used for defuzzification. By this method, the value of fuzzy output which has the maximum possibility distribution is used as control output.

4 Simulation Results

The objectives of the carried out simulations are to show the dynamic performances of the proposed control strategy. DTC with three-level inverter and the system with a Fuzzy Logic controller for the inverter state selection have been simulated to make comparison. The specifications of the electric vehicle load and the induction motor are given in **Table 2**.

Table 2

Specifications of the electric vehicle load and the induction motor.

Length	5m
Width	2m
Height	1m
Wheelbase	2.4m
Weight	250kg
Aerodynamic drag coefficient	0.12
Rolling resistance coefficient	0.005
Wheel	2 in the front 2 to the rear
Rotational inertia	1.1
Wheel radius	0.29m
Induction motor	2kw, 380V, p = 2, 20Nm, 50Hz
Rotor resistance	1.8 Ω
Rotor inductance	0.1568H
Stator resistance	1.2 Ω
Stator inductance	0.1558H
Mutual inductance	0.15H
Moment of inertial	0.07kgm ²

Figs. 7a, 7b and 7c show the torque response, the motor currents and flux response respectively (for step), without FLC.

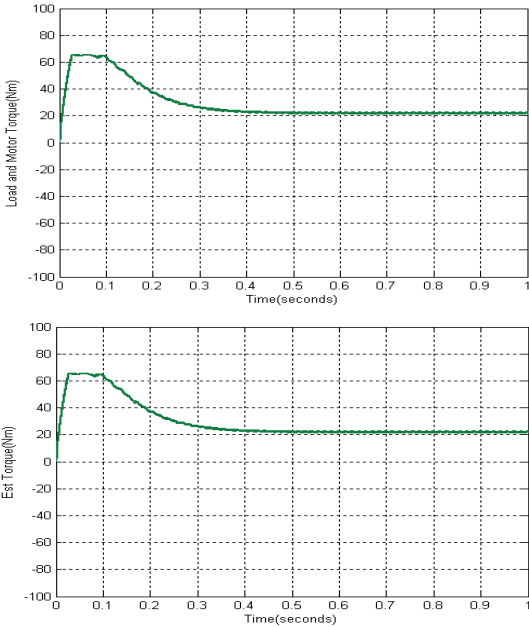


Fig. 7a – Torque response of vehicle motor (for step), without FLC.

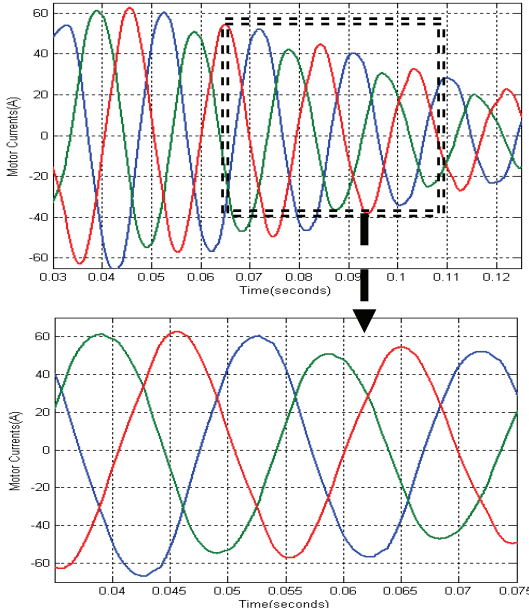


Fig. 7b – Motor current response of vehicle motor (for step), without FLC.

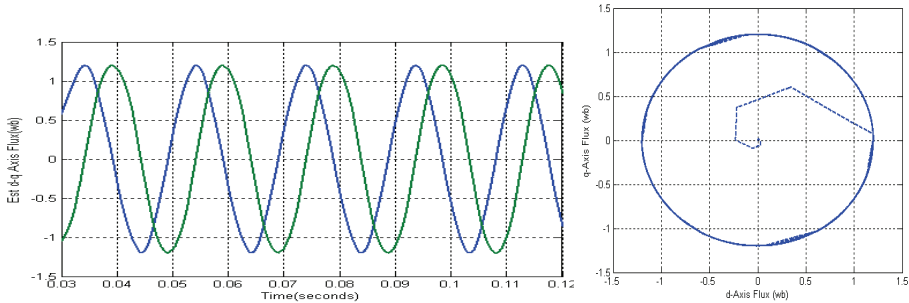


Fig. 7c – Flux response of vehicle motor (for step), without FLC.

Figs. 8, 9 and 10 show the torque response, the motor currents and flux response respectively (for step), with FLC. The electric dynamics vehicle is shown in Figs. 9 and 10. Figs. 11, 12 and 13 show the speed response, torque response and flux response respectively during starting, acceleration and deceleration (Regenerative braking), without FLC. Figs. 14, 15 and 16 show the speed response, torque response and flux response respectively during starting, acceleration and deceleration (Regenerative braking), with FLC. The results demonstrate that FLC based DTC reduces the current ripples and large torque.

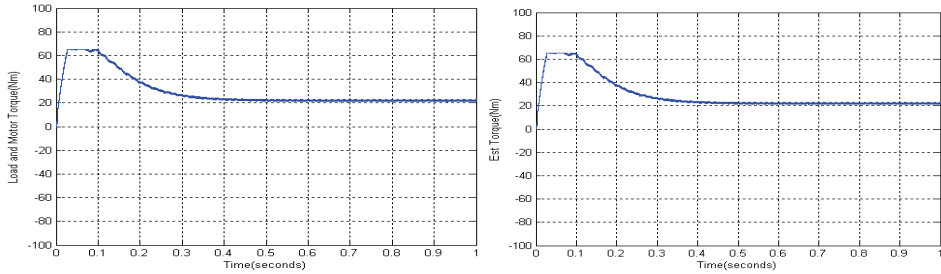


Fig. 8 – Torque response of vehicle motor (for step), with FLC.

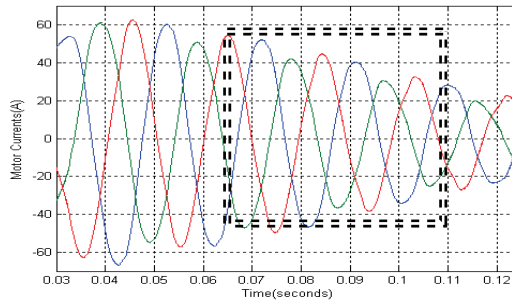


Fig. 9a – Motor current response of vehicle motor (for step), with FLC

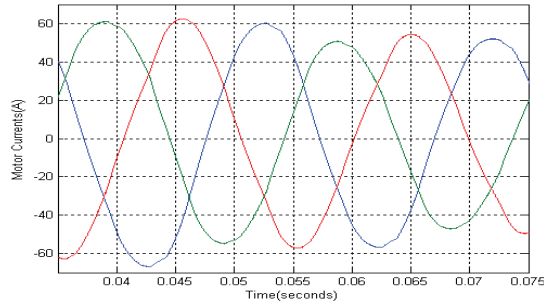


Fig. 9b – Enlarged part of Fig. 9a.

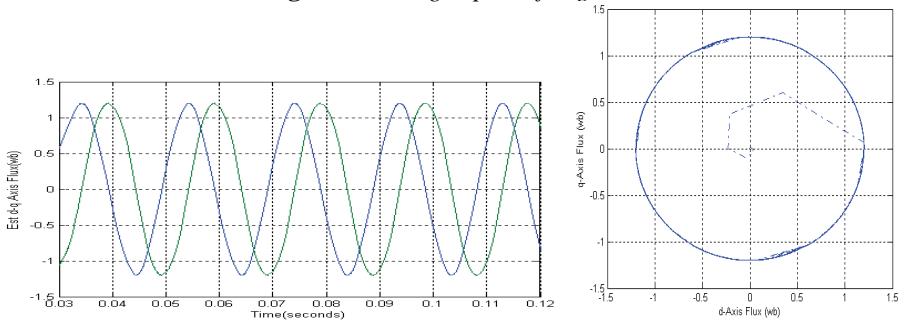


Fig. 10 – Flux response of vehicle motor (for step), with FLC.

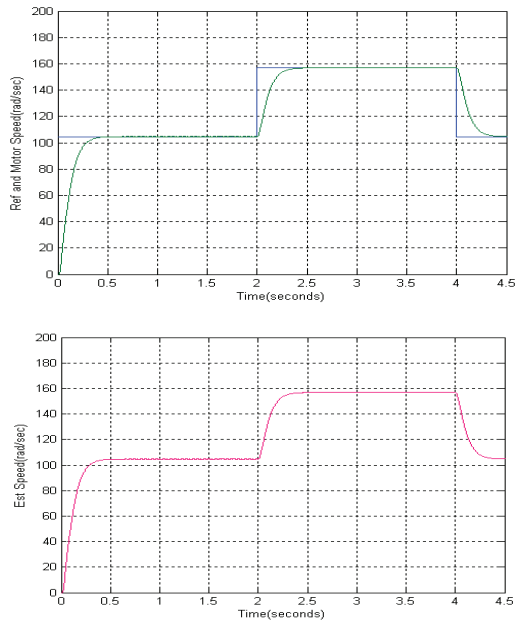


Fig. 11 – Speed response of vehicle motor during starting, acceleration and deceleration (Regenerative braking), without FLC.

Improve the DTC System for Electric Vehicles Induction Motors

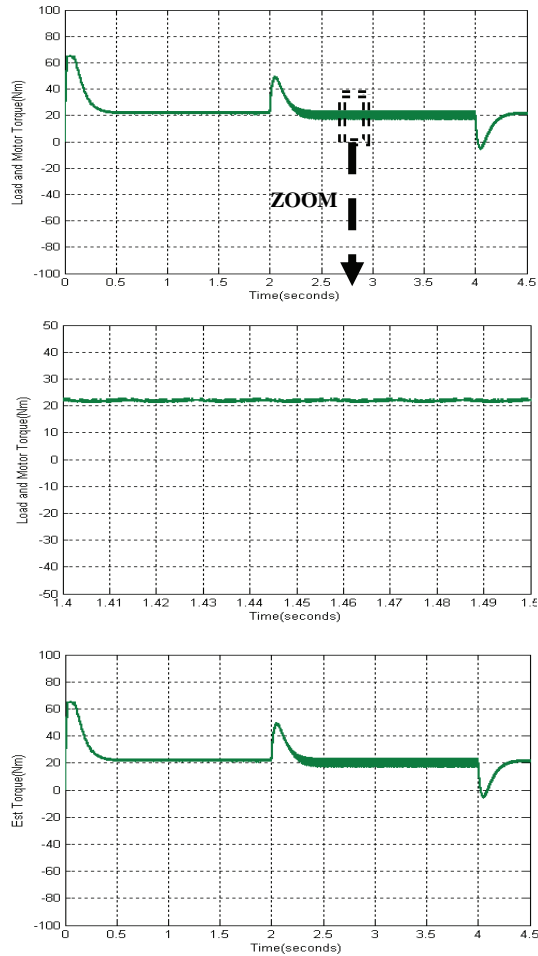


Fig. 12 – Torque response of vehicle motor during starting, acceleration and deceleration (Regenerative braking), without FLC.

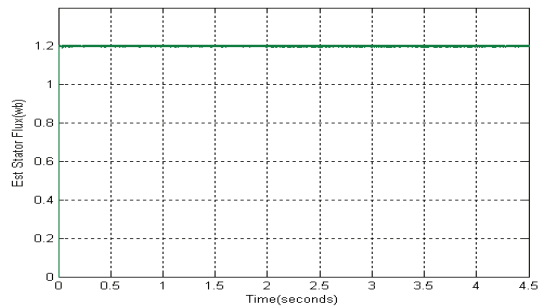


Fig. 13 – Flux response of vehicle motor during starting, acceleration and deceleration (Regenerative braking), without FLC.

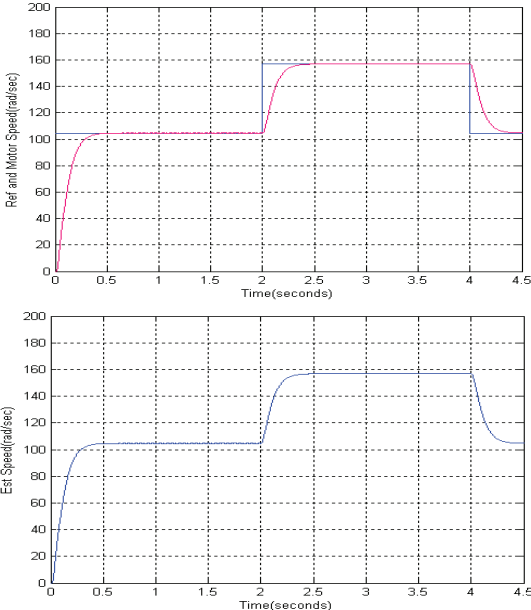


Fig. 14 – Speed response of vehicle motor during starting, acceleration and deceleration (Regenerative braking), with FLC.

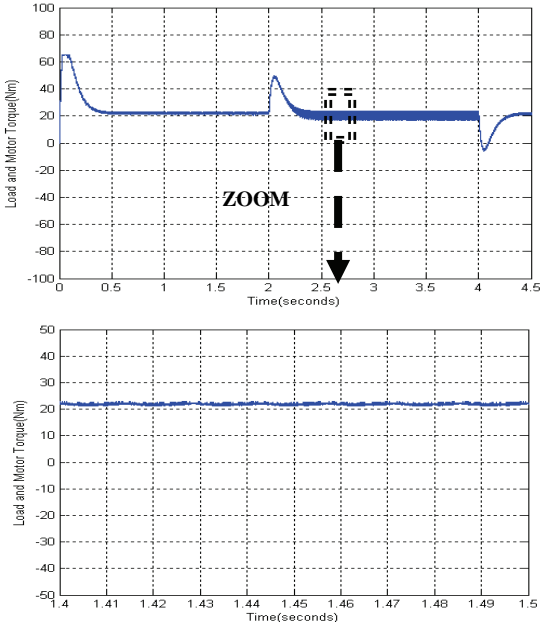


Fig. 15b – Torque response of vehicle motor during starting, acceleration and deceleration (Regenerative braking), with FLC.

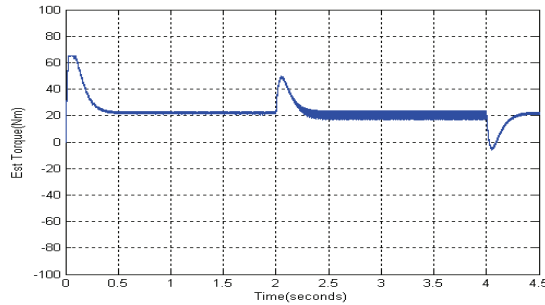


Fig. 15b – Torque response of vehicle motor during starting, acceleration and deceleration (Regenerative braking), with FLC.

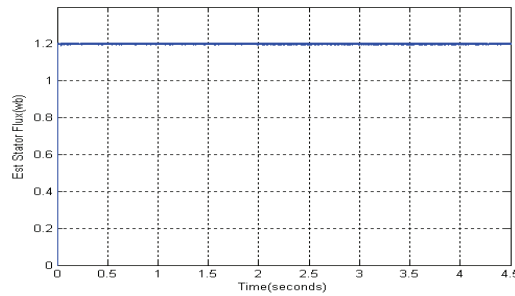


Fig. 16 – Flux response of vehicle motor during starting, acceleration and deceleration (Regenerative braking), with FLC.

5 Conclusion

The performance of FLC based DTC induction motor drive strategy has been compared with the conventional method based on a table. There is approximately 35% reduction in torque and current ripple in fuzzy logic controller based DTC scheme. A simulations test of the proposed strategy (aerodynamics vehicle and DTC with FLC) provides a good dynamic response.

6 Nomenclature

v – Vehicle speed;	α – Grade angle;
f_{ad} – Aerodynamic drag or viscous resistance;	f_{ad} – Aerodynamic drag force;
f_r – Rolling resistance force;	F_w – Road load;
m – Vehicle mass;	Φ_s – Stator flux;

f	– Tire rolling resistance coefficient	f_{rs}	– Climbing resistance force
g	– Gravitational acceleration constant;	C_w	– Aerodynamic drag coefficient;
ξ	– Air density;	Φ_r	– Rotor flux;
R_r	– Rotor resistance;	R_s	– Stator resistance;
A	– Vehicle frontal area;	L_s	– Stator inductance;
v_0	– Head-wind velocity;	L_r	– Rotor inductance;
F_{tr}	– Motive force;	L_m	– Mutual inductance;
J	– Total inertia (of the system);	ω_r	– Rotor electric speed;
T_{ev}	– Electric vehicle torque;	B	– Viscous coefficient.
T_e	– Motor torque;	P	– Pole-pair number;
r_{wh}	– Wheel radius;	ω	– Angular velocity;
V_r	– Rotor voltage;	V_s	– Stator voltage;
θ_s	– Stator flux angular position;		

7 References

- [1] U. Baader, M. Depenbrock, G. Gierse: Direct Self Control (DSC) of Inverter Fed Induction Machine: A Basis for Speed Control without Speed Measurement, IEEE Transaction on Industry Applications, Vol. 28, No. 3, May/June 1992, pp. 581 – 588.
- [2] O. Kukrer: Discrete-time Current Control of Voltage-fed Three-phase PWM Inverter, IEEE Transaction on Power Electronics, Vol. 11, No. 2, March 1996, pp. 260 – 269.
- [3] M. Vasudevan, R. Arumugam, S. Paramasivam: High-performance Adaptive Intelligent Direct Torque Control Schemes for Induction Motor Drives, Serbian Journal of Electrical Engineering, Vol. 2, No. 1, May 2005, pp. 93 – 116.
- [4] I. Takahashi, T. Noguchi: A New Quick-response and High Efficiency Control Strategy of an Induction Motor, IEEE Transaction on Industrial Applications, Vol. IA-22, No. 5, Sept. 1986, pages 820 – 827.
- [5] A. Nabae, I. Takahashi, H. Akagi: A New Neutral-point-clamped PWM Inverter, IEEE Transaction on Industrial Applications, Vol. IA-17, No. 5, Sept 1981, pp. 518 – 523.
- [6] K.B. Lee, J.H. Song, I. Choy, J.Y. Yoon: Torque Ripple Reduction in DTC of Induction Motor Driven by Three-level Inverter with Low Switching Frequency, IEEE Transaction on Power Electronics, Vol. 17, No 2, March 2002, 255 – 264.

Improvement the DTC System for Electric Vehicles Induction Motors

- [7] X. Hu, L. Zhang: A Predictive Direct Torque Control Scheme for a Three-level VSI-fed Induction Motor Drive, 9th International Conference on Electrical Machines and Drives, Canterbury, UK, 1999, pp. 334 – 338.
- [8] X. Wu, L. Huang: Direct Torque Control of Three-level Inverter using Neural Networks as a Switching Vector Selection, 36th IAS Annual Meeting, IEEE Industry Applications Society, Vol. 2, Chicago, IL, USA, Sept/Oct. 2001, pp. 939 – 944.
- [9] A. Haddoun, M.E.H. Benbouzid, D. Diallo, R. Abdessemed, J. Ghouili, K. Srairi: A Loss-minimization DTC Scheme for EV Induction Motor, IEEE Transaction on Vehicular Technology, Vol. 56, No. 1, Jan. 2007, pp. 81 – 88.
- [10] F. Khoucha, K. Marouani, A. Kheloui, K. Aliouane: Experimental Performance Analysis of Adaptive Flux and Speed Observers for Direct Torque Control of Sensorless Induction Machine Drives, IEEE 35th Power Electronics Specialists Conference PESC 2004, Vol. 6, Aachen, Germany, June 2004, pp. 2678 – 2683.
- [11] M. Ehsani, K.M. Rahman, H.A. Toliyat: Propulsion System Design of Electric and Hybrid Vehicles, IEEE Transaction on Industrial Electronics, Vol. 44, No. 1, Feb. 1997, pp 19 – 27.
- [12] I. Husain, M.S. Islam: Design, Modeling and Simulation of an Electric Vehicle System, International Congress and Exposition Detroit, MI, USA, SAE Technical Paper Series, Paper No. 1999-01-1149, March 1999.
- [13] V. Perelmuter: Three-level Inverters with Direct Torque Control, IEEE Industry Applications Society Annual Meeting, Vol. 3, Rome, Italy, Oct. 2000, pp. 1368 – 1374.
- [14] R. Zaimeddine, E.M. Berkouk, L. Refoufi: A Scheme of EDTC Control using an Induction Motor Three-level Voltage Source Inverter for Electric Vehicles, Journal of Electrical Engineering and Technology, Dec. 2007, Vol. 2, No. 4, pp. 505 – 512.
- [15] K. Bousserhane, A. Hazzab, M. Rahli, B. Mazari, M. Kamli: Position Control of Linear Induction Motor using an Adaptive Fuzzy Integral-backstepping Controller, Serbian Journal of Electrical Engineering, Vol. 3, No. 1, June 2006, pp. 1 – 17.
- [16] S.A. Mir, D.S. Zinger, M.E. Elbuluk: Fuzzy Controller for Inverter Fed Induction Machines, IEEE Transaction on Industry Applications, Vol. 30, No. 1, Jan/Feb. 1994, pp. 78 – 84.
- [17] M. Kadjoudj, N. Golea, M.E. Benbouzid: Fuzzy Rule-based Model Reference Adaptive Control for PMSM Drives, Serbian Journal of Electrical Engineering, Vol. 4, No. 1, June 2007, pp.13 – 22.